Wave propagation and optical properties in slabs with light-induced free charge carriers

Alberto Lencina
Departamento de Física, Universidade Federal da Paraíba, Caixa Postal 5008 CEP 58051-970, João Pessoa, Paraíba, Brazil

Pablo Vaveliuk*
Departamento de Física, Universidade Estadual de Feira de Santana, Campus Universitário, BR 116, KM 03, Feira de Santana 44031-460, Bahia, Brazil

Beatriz Ruiz, Myrian Tebaldi, and Néstor Bolognini
Centro de Investigaciones Ópticas, cc 124 (1900), La Plata, Buenos Aires, Argentina
(Received 6 April 2006; revised manuscript received 29 June 2006; published 30 November 2006)

A theoretical analysis on wave propagation and optical properties of slabs with light-induced free charge carriers within a Fabry-Pérot framework is presented. The key of the analysis is to attack the wave propagation problem in terms of the time-averaged Poynting vector modulus within the medium through an alternative approach. This fact allows coupling the microscopic (free charge rate) and macroscopic (electromagnetic field evolution) equations self-consistently by means of the nonlinear permittivity and conductivity, which, in turn, depend on the time-averaged Poynting vector modulus. Thereby, the transmittance, reflectance, and absorptive power are derived as functions of the pump intensity and medium thickness. Bistable behavior is found at relatively high excitation intensity for positive values of the nonlinear permittivity coefficient. The bistability enhances for increasing values of such coefficient and weakens for increasing values of nonlinear photoconductivity coefficient. On the contrary, for negative nonlinear permittivity coefficient, bistability does not appear possessing these media mirrorlike behavior. Some possible applications are suggested.

DOI: 10.1103/PhysRevE.74.056614 PACS number(s): 42.25.Bs, 42.70.Nq, 42.65.Pc

I. INTRODUCTION

Light-induced free-charge-carrier media is a general denomination employed for materials in which an appropriate illumination produces free electrons, free holes, or both whose characteristics depend on both the material energy band structure and the energy of the radiation quanta. The study of these materials increased considerably in the last decades due to their wide range of applications in optoelectronics, for example, passive optical limiting [1–3], xerographic processes [4–6], and visible and IR detection [7–11] with materials ranging from semiconductors [1,2,10,11] to insulators [3,12–16] passing also by organic materials [17,18].

The processes involving light-induced free charges, as generation, recombination, and interaction with photons and other particles and quasiparticles, produce changes in the medium optical response. This response could be divided in two nonindependent parts: light-induced absorption and free-charge-carrier refraction. Both phenomena strongly depend on the photoinduced free-charge-carrier density in the whole volume of the material which, in turns, depend on the radiation intensity distribution in it. Therefore, from an electromagnetic point of view, it is a nonlinear optical phenomenon. A proper analysis requires the use of the microscopic semiclassical theory for the free-charge-carriers evolution through rate equations together with macroscopic Maxwell's equations for the light field. The appropriate boundary conditions and phenomenological constitutive relations must be also considered. The set of macroscopic-microscopic equations constitutes an adequate approach to describe the optical properties of the material. However, this set could result in a very complex mathematical problem due to the strong coupling between the free charge density and the radiation intensity inside the medium. To avoid this difficulty, in some cases the real intensity is replaced by an averaged intensity and the field equations are also simplified within the well-known slowly varying envelope approximation [19]. In other situations, the microscopic processes are prioritary, thereby placing the optical excitation only as a parameter [4,5,9,10,18], or the macroscopic optical response is the principal issue and the microscopic processes are oversimplified [14,20,21].

Recently an approach, the so-called S-formalism [22], was developed to study the plane wave propagation through parallel-plane-face media. The S-formalism replaces the field variables, i.e., the electric field amplitude modulus and phases of forward and backward counterpropagating waves, by a general electric field amplitude modulus and the total time-averaged Poynting vector modulus. This method allows knowing, point to point, the time-averaged Poynting vector within the medium once the evolution equations were resolved. Therefore, when the nonlinearity has a direct relationship on the time-averaged Poynting vector and the medium is nonconservative, i.e., the reflectance plus transmittance lesser than the unity, the S-formalism seems proper to solve the macroscopic problem. The light-induced free-charge-carriers media are a particular case of these nonlinear phenomena. Then, the transmittance, reflectance, and absorptive power in terms of the excitation intensity and slab thickness for different nonlinear permittivities and conductivities are studied within this framework. Different behaviors appear pointing out the bistability, as in others nonlinear slabs

*Corresponding author. E-mail address: pablov@fisica.ufpb.br

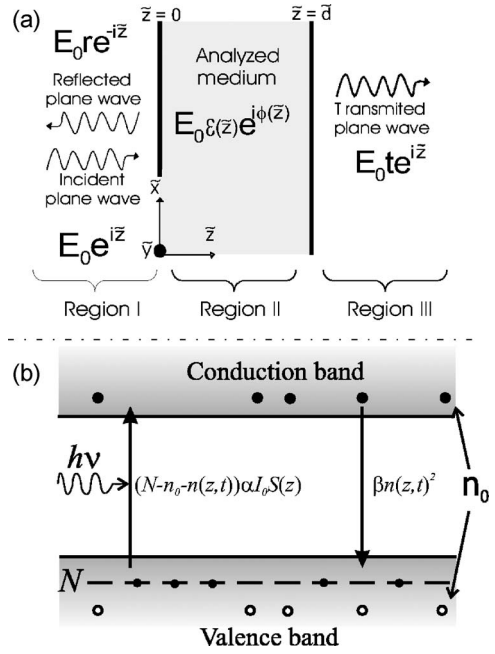

FIG. 1. (a) A harmonic plane wave of amplitude E_0, impinges on a parallel-plane-faces medium surrounded by vacuum. The wave is reflected and transmitted with coefficients r and t, respectively, without changes in its polarization. Note that, $\tilde{z}=k_0z$ is the dimensionless propagation coordinate. (b) Schematic representation of the intrinsic interband transitions problem. Electrons are excited from the valence band to form an electron-hole pair.

[22,23], and mirrorlike behavior. The conditions in which these behaviors occur strongly depend on the nonlinear conductivity and permittivity coefficients.

The macroscopic and microscopic equations are presented in Sec. II, showing the advantages to utilize the S-formalism. The principal results from the model are given and discussed in Sec. III. Finally, in Sec. IV, we establish the conclusions.

II. MACROSCOPIC-MICROSCOPIC MODEL

In this section, we present the relevant macroscopic and microscopic equations, which are linked by the time-averaged Poynting vector modulus. The S-formalism [22] provides the framework to know the evolution of the time-averaged Poynting vector modulus.

A. Light field equations

The problem to be analyzed is schematized in Fig. 1(a). It considers a harmonic and linearly polarized plane wave of frequency ω and wave vector $\mathbf{k}_0$. This wave impinges perpendicularly in a nonmagnetic, homogeneous, isotropic, and spatially nondispersive medium (region II) surrounded by vacuum (for simplicity). The dimensionless thickness is $\tilde{d}=k_0d$ being d, the slab thickness. The optical field maintains constant its polarization so that a scalar approach is valid. The incident wave is reflected and transmitted with amplitudes rE_0 and tE_0 where r and t are the complex reflection and transmission coefficients, respectively. The field structure in region II is $E_{II}=E_0\mathcal{E}(\tilde{z})\exp[i\phi(\tilde{z})]$, where $\mathcal{E}$ and ϕ are the real dimensionless amplitude and phase, respectively. The equations that govern the wave propagation in terms of $\mathcal{E}$ and the dimensionless variable, $S=\mathcal{E}^2d\phi/d\tilde{z}$ result [22]

$$\frac{d^2\mathcal{E}}{d\tilde{z}^2}+\epsilon_t(\tilde{z};S)\mathcal{E}-\frac{S^2}{\mathcal{E}^3}=0, \tag{1a}$$

$$\frac{dS}{d\tilde{z}}+\sigma_t(\tilde{z};S)\mathcal{E}^2=0, \tag{1b}$$

where $\tilde{z}$ is the dimensionless propagation coordinate, and ϵ_t and σ_t are the total dimensionless permittivity and the total dimensionless conductivity, respectively. These dimensionless parameters contain the linear as well as the nonlinear response of the medium.

The field variable S is directly related with the time-averaged Poynting vector modulus $|\langle\mathbf{S}\rangle|$ along each point $\tilde{z}$ within the slab through the expression

$$S(\tilde{z})=\frac{1}{I_0}\langle\mathbf{S}(\tilde{z})\rangle\cdot\hat{\mathbf{u}}_z \tag{2}$$

where $I_0=\epsilon_0\omega/(2k_0)E_0^2$ is the incident intensity with ϵ_0, the vacuum permittivity and $\hat{\mathbf{u}}_z$ the unit vector in the z direction.

Macroscopically, ϵ_t and σ_t depend on the field variables $(\mathcal{E},S)$ through the constitutive relations. Microscopically, ϵ_t and σ_t depend on the free-charge-carrier density. The simplest form of this dependence is given by the classical Drude-Lorentz model of harmonic oscillators [24]. In turn, the free charge carriers density depends on S through the free-charge-carrier rate equation raised from the energy band structure of the material.

B. Constitutive relations

The constitutive relations are the phenomenological relations that take into account the medium response to the electromagnetic fields through the macroscopic dimensionless parameters ϵ_t and σ_t. The structure of the parameters has a linear part being $\tilde{\epsilon}_1=\epsilon_1/\epsilon_0$ with ϵ_1, the dielectric constant and $\tilde{\sigma}_1=\sigma_1/(\epsilon_0\omega)$ with σ_1, the ohmic conductivity, together with a nonlinear photoinduced part that according to the simplest Drude-Lorentz microscopic model [24] are linear with the free-charge-carrier density n being able to be written as

$$\epsilon_t=\tilde{\epsilon}_1+\gamma n_0\frac{n(\tilde{z};S)}{n_0}, \tag{3a}$$

$$\sigma_t=\tilde{\sigma}_1+\delta n_0\frac{n(\tilde{z};S)}{n_0}, \tag{3b}$$

where γ and δ are the medium nonlinear permittivity and conductivity coefficients, respectively, and n_0 is the thermally excited density of centers. The convenience of introducing this parameter is due to the fact that the numerical simulations will be performed in terms of dimensionless parameters. The expressions of γn_0 and δn_0 in terms of microscopic parameters for one-photon absorption can be found in

Ref. [25]. In general, γn_0 can be written as $\gamma n_0 = 4\pi q^2 n_0 f(\omega;\omega_g)/m^*$ being q, the electron charge, m^*, the reduced effective electron-hole mass and ω_g, the gap angular frequency. The function $f(\omega;\omega_g)$ represents the structure function of the interband transition and depends on the particular model assumed in the analysis. For example, in the case of the simplest Drude-Lorentz model, it is given by $f_{DL}(\omega;\omega_g)=\omega^{-2}[\omega_g^2/(\omega^2-\omega_g^2)]$. In spite of the fact that $f(\omega;\omega_g)$ for real light-induced free-charge-carrier materials is certainly more complex than $f_{DL}(\omega;\omega_g)$, this model provides a general description that could give us a first insight into the principal features for interband transitions. The function $f_{DL}(\omega;\omega_g)$ produces a positive γn_0 for $\omega > \omega_g$, and negative otherwise. However, this structure function is very restrictive for nonresonant transitions because of its narrow bandwidth. Models with larger bandwidth are obtained through the inclusion of a damped term in the Drude-Lorentz expression and a mean-field correction, both necessary to describe dense media. On the other hand, δn_0 could be related with the mobility of electrons μ_e and holes μ_h through $\delta n_0 = q n_0(\mu_e+\mu_h)/\epsilon_0\omega$.

C. The free-charge-carrier rate equation

The light-induced free-charge-carrier density n depends on the energy flux in each point $\tilde{z}$ of the medium. The functional form of such dependence can be derived from a semiclassical scheme considering the energy band structure and the dynamic process that occurs in the medium due to the interaction with the radiation field. The microscopic processes considered in this work are those corresponding to intrinsic interband transitions [4–6,26] schematized in Fig. 1(b). Although the model is very simple, it exhibits the main features of this kind of media. Extensions to more complicated situations are straightforward to carry out; for example, in the case of extrinsic transitions the model is included in Appendix. For intrinsic interband transitions, the processes considered are: (i) the generation of electron-hole pairs (with probability α) from a finite number of centers $(N-n_0)$, with N the total density of centers able to be excited and n_0 the thermally excited ones, and (ii) the recombination of electron-hole pairs through *bimolecular recombination* [5,6] with probability β. These processes are expressed by the following rate equation:

$$\frac{dn(\tilde{z},S)}{dt} = [N - n_0 - n(\tilde{z},S)]\alpha I_o S(\tilde{z}) - \beta n^2(\tilde{z},S). \tag{4}$$

Equation (4) represents the temporal-averaged rate equation. The average is justified by two reasons: (i) we are not taken into account the thermal noise [9], i.e., thermal-induced pair variations that could generate high-frequency variations in the light-induced free-charge-carrier density n (n_0 is constant in our analysis); and (ii) we are interested in the average variations of n and not in their fluctuations [4,27]. Besides, the model described by Eq. (4) only considers the one-photon interband transitions. Models of hot electrons [11] and two-photon absorption [2,3,21] do not concern us. The diffusion of free charges could be considered by adding to Eq. (4) the term $k_0 D\partial^2 n/\partial\tilde{z}^2$, where D is the diffusion constant. It will be shown in Sec. III that the diffusion is negligible when compared to the recombination term within the parameter range considered. Therefore, it can be neglected in our analysis. For the steady state, $d/dt=0$ so that

$$\frac{n(\tilde{z})}{n_0} = \xi S(\tilde{z})\left(\sqrt{1+\frac{2(N_0-1)}{\xi S(\tilde{z})}}-1\right), \tag{5}$$

where $\xi = \alpha I_o/(2\beta n_0)$ is the *dimensionless excitation parameter* and $N_0 = N/n_0$ is the relative density of photoexcitable atoms. Then, the relative density of light-induced pairs can be studied in term of two dimensionless parameters: ξ and N_0.

D. Optical properties

From Eqs. (1), (3), and (5), the optical properties of the medium (i.e., the reflectance R, transmittance T, and absorptive power A [28,29]) can be deduced. In fact, by replacing Eq. (5) into (3) and, in turn, Eqs. (3) into (1) and considering the corresponding boundary conditions [22],

$$\left[(\mathcal{E}^2+S)^2 + \left(\mathcal{E}\frac{d\mathcal{E}}{d\tilde{z}}\right)^2 - 4\mathcal{E}^2\right]_{\tilde{z}=0} = 0, \tag{6a}$$

$$[S-\mathcal{E}^2]_{\tilde{z}=\tilde{d}} = 0, \tag{6b}$$

$$\left[\frac{d\mathcal{E}}{d\tilde{z}}\right]_{\tilde{z}=\tilde{d}} = 0, \tag{6c}$$

where $0 \le S, \mathcal{E} \le 1$, it gives R, T, and A in terms of S at $\tilde{z}=0$ and $\tilde{z}=\tilde{d}$ by the following expressions:

$$R = |r|^2 = 1 - S(0), \tag{7a}$$

$$T = |t|^2 = S(\tilde{d}), \tag{7b}$$

$$A = S(0) - S(\tilde{d}). \tag{7c}$$

Thereby, all the optical measurable quantities are related to the boundary values of the dimensionless time-averaged Poynting vector, emphasizing the strength of the S-formalism to self-consistently solve the wave propagation problem in this type of media.

III. RESULTS AND DISCUSSION

To study the wave propagation and optical properties of the light-induced free-charge-carrier media, Eqs. (1) were solved numerically. The total permittivity and conductivity are given by Eqs. (3), and the free charge carriers depends on the time-averaged Poynting vector modulus according to Eq. (5). The two first boundary conditions [Eqs. (6a) and (6b)] give a relation between S and $\mathcal{E}$ at the boundaries whereas the last condition [Eq. (6c)] fixes a value for the derivative of $\mathcal{E}$. This fact makes difficult the numerical implementation in order to guarantee the unicity of the solution. To overcome this difficulty, we assigned in Eq. (6b) a value m between 0

and 1 to $S(\tilde{d})$ and $\mathcal{E}(\tilde{d})$. Then, to find the true m value satisfying Eq. (6a), we solve Eqs. (1) by a fourth-order Runge-Kutta method. Once the self-consistent system was resolved, $S(\tilde{z})$ was evaluated at the boundaries $\tilde{z}=0$ and $\tilde{z}=\tilde{d}$, such that T, R, and A can be obtained from Eqs. (7) in terms of the dimensionless excitation parameter ξ and the slab thickness $\tilde{d}$. Under dark conditions, the medium is assumed to be insulator so that σ_1 was taken zero. We used the following values for the dimensionless parameters: $N_0=10^{12}$, $n_0\delta=10^{-5}$, 10^{-4}, and $|n_0\gamma|=0$, 10^{-3}. A link between the physical parameters that characterize the linear, as well as nonlinear properties, of real materials with these dimensionless parameters used by us is thought to be necessary in order to verify that the simulations carried out in the manuscript are physically feasible. There is a large amount of experimental data for semiconductors and photoconductors that can be considered, as an example, from Ref. [30]. The value of N_0 is feasible when compared to different values of several materials from [30]. The value used in the simulations is close to the InP and GaSb. On the other hand, by considering that the optical angular frequencies are around 10^{15} Hz, the nonlinear coefficient δn_0 varies from 10^{-11} to 10^2 considering six typical materials: InSb, GaAs, InP, InAs, GaSb, and Si. Therefore, our simulations present an intermediate value in relation to the considered materials. From [30], it is observed that for InSb, the nonlinear absorption could be important, whereas for GaAs, Si, and InP, it becomes negligible. Furthermore, the values for GaSb and InAs are very close to the values employed in our simulations. For the dimensionless nonlinear refraction γn_0, the values that could be obtained from [30] are strongly dependent on the structure function $f(\omega;\omega_g)$ considered for the optical transition. This fact makes it difficult to compare those values calculated from [30] with the values used in our simulations. The Drude-Lorentz model seems to be inappropriate because of its narrow bandwidth. However, wide-bandwidth models corresponding to real photoconductors, could place the nonlinear refraction coefficient that we used as an intermediate value.

To deepen the analysis, we define the spatially averaged permittivity by

$$\langle \epsilon_t \rangle = \frac{1}{\tilde{d}} \int_0^{\tilde{d}} \epsilon_t d\tilde{z}. \tag{8}$$

This magnitude behaves as the *effective* permittivity and have a direct relation with the optical properties R, T, and A.

We first analyze the dependence of R, T, and A on the dimensionless excitation parameter. The analysis was done for a fixed slab thickness, a fixed linear susceptibility, and several values of the nonlinear coefficients, $n_0\gamma$ and $n_0\delta$. The results of our calculi are summarized in Fig. 2 placed in matrix form with each subfigure representing a set of $(n_0\gamma, n_0\delta)$ values where top, center and bolttom stands for $n_0\gamma=0$, $n_0\gamma>0$, and $n_0\gamma<0$, respectively; and left and right stands for $n_0\delta=10^{-5}$ and $n_0\delta=10^{-4}$. For $n_0\gamma=0$ (Fig. 2, top), the averaged permittivity is given by their linear value, $\langle \epsilon_t \rangle = \epsilon_1$. This is a limiting case since the free charge generation will not imply variations in the effective permittivity. It is observed a completely bijective behavior for R, T, and A in terms of ξ. For this pure light-induced absorption process, the transmittance decreases monotonically as ξ increases for all values of $n_0\delta$. When $n_0\delta$ increases the transmittance continues monotonically decreasing, with a marked slope. However, the reflectance holds quasi-negligible along the considered ξ range, such as the transmittance decreasing is produced exclusively by the irreversible electromagnetic energy transfer to the medium. The light-induced free-charge-carrier density is a function of the time-averaged Poynting vector and, in this case, to first-order Eq. (5) is proportional to $\sqrt{S(z)}$ so that is expected that the photoconductivity behaves in a similar way. This behavior was obtained in the photoconductivity measurements for interband transitions in photorefractive materials [16].

A completely different behavior is observed for $n_0\gamma \neq 0$, i.e., when the spatial-averaged permittivity is altered by the free-charge-carrier density variation. For $n_0\gamma>0$ (Fig. 2, center) and low values of the ξ range considered, the transmittance decreases monotonically, as displayed in Fig. 2, center, left. As the dimensionless excitation parameter increases, the spatially averaged permittivity increases to produce greater impedance mismatch between the slab and the surrounding medium. Then, the reflectivity increases as far as T decreases and the absorptive power remains negligible. However, as ξ continues increasing, oscillatory behavior and bistability appear for R, T, and A, which is related to the appearing of bistable behavior in the average permittivity. Optical bistability by light-induced free-charge-carrier processes was experimentally observed, for example, in InSb [31] and InAs [32]. In both cases, radiation energy was greater than band-gap energy. This type of transitions are macroscopically described by a positive γn_0, being then consistent with the results of the present analysis. It is well known from a theoretical point of view that optical bistability can occurs by combining material nonlinearity with additional feedback [19]. Similar bistable behavior in the transmittance in terms of nonlinear parameter was shown in Kerr [23] and Poynting media [22] without losses. On the contrary to these media, in Fig. 2, the peaks in T do not reach the value 1 when ξ increases due to the energy absorption. The bistable behavior can be understood by remembering that the nonlinearity behaves approximately as $\sqrt{S(z)}$, and the phenomenon appears as produced by a "fractional Poynting medium" [22]. Also, the feedback effect produced by the Fabry-Pérot geometry is essential to producing such a phenomenon. It was shown, for example, in Ref. [23], that the bistability disappears when the medium become semi-infinite ($\tilde{d}\to\infty$) even for very intense nonlinearities. By observing Fig. 2, center, right it is apparent that the optical properties change with respect to those depicted in Fig. 2, center, left. The bistable behavior disappear when ξ increases and, even if attenuated, R, T, and A maintain their oscillatory behavior. When $n_0\delta$ increases, the bistability and oscillations attenuation, in R, T, and A shows that these effects are inherent to the refractive properties of the medium rather than to the absorptive-dissipative process. This is an important feature of this kind of media for practical applications, such as op-

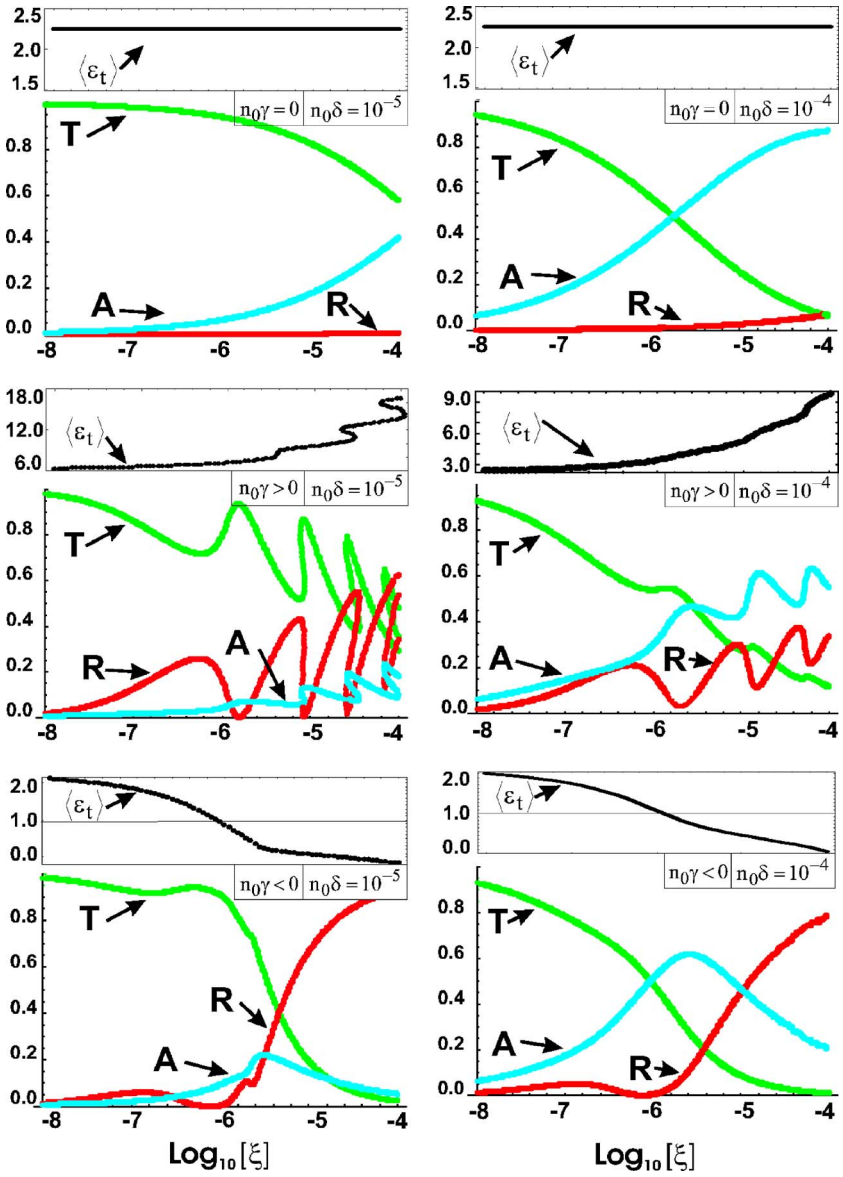

FIG. 2. (Color online) Transmittance, reflectance, absorptive power, and spatially averaged generalized relative permittivity as function of the dimensionless excitation parameter for several $(n_0\gamma, n_0\delta)$ values as indicated in each graph. All figures with $\epsilon_1=2.25$ and $\tilde{d}=2\pi$.

tical switches. The result predicts that the light-induced absorption should be controlled in order to maintain the bistability.

Another interesting case corresponds to $n_0\gamma<0$ (Fig. 2, bottom), where a completely different behavior occurred. In this situation, the medium response is in "quadrature" with the optical excitation and the value of the medium polarizability turns out negative. As depicted in Fig. 2, bottom the transmittance begins diminishing in a similar form that for the case $n_0\gamma=0$. Remember that, in Fig. 2, top, $\langle\epsilon_t\rangle$, R, T, and A do not present bistable behavior. Also, the oscillatory behavior in the optical properties is not present in these optical properties in Fig. 2, bottom . However, our simulations confirms that the oscillatory behavior appears and became more intense when the linear permittivity increases. On the other hand, bistability does not appear confirming that is not related with negative values of $n_0\gamma$. By comparing both figures, it is clear that any oscillatory behavior of R, T, and A, when $n_0\delta$ increases, will also be ironed out as in the $n_0\gamma>0$ case. On the other hand, for low ξ values, T reaches its highest values, decreasing as far as ξ increases, while R and A are close to zero. Nevertheless, the behavior of the optical properties changes dramatically in the ξ region for which $\langle\epsilon_t\rangle\approx 1$. The absorptive power presents a peak whose strength increases when $n_0\delta$ increases. Furthermore, in the *transition* region the transmittance and reflectance exhibits an opposite behavior, increasing the former and decreasing the later. Still increasing ξ, the reflectance value tends to one and T and A tend to zero. Thus, the medium presents a *mirrorlike* behavior for higher ξ values. Recall that, no absorption occurs in the medium and all the light is reflected. This very interesting result could lead to the construction of light-induced mirror devices. These mirrors could be induced through the incident intensity variation or by increasing the medium temperature and modifying thereby the recombination probability. Note that the results of Fig. 2, bottom indicate that the mirrorlike behavior is more efficient for lower nonlinear conductivity variations. There are some experimental results that could be explained in terms of a negative nonlinear permittivity important to building light-induced

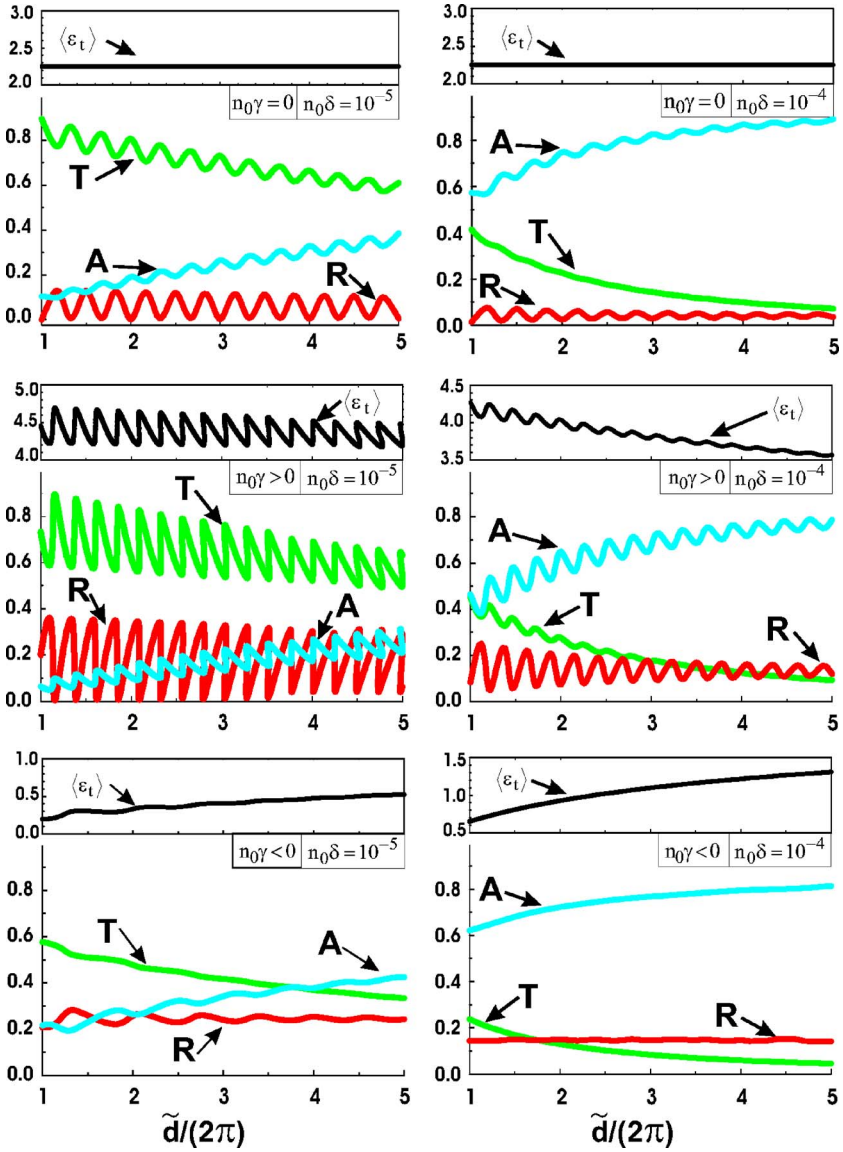

FIG. 3. (Color online) Transmittance, reflectance, absorptive power, and spatially averaged generalized relative permittivity as function of the dimensionless thickness for several $(n_0\gamma, n_0\delta)$ values as indicated in each graph. All figures with $\epsilon_1=2.25$ and $\ln_{10}\xi=-5.5$.

mirror devices. These experiments deal with optical limiting properties of Si [33] and GaP [34] when illuminated by picosecond light pulses of $\lambda=1064$ nm and $\lambda=532$ nm, respectively. Interestingly, for each material, the energy of the used radiation is located above the threshold for indirect interband transitions but below the energy need to account a direct transition. Then, interband transitions at these wavelengths should provide $\gamma n_0<0$ because $\omega<\omega_g$. Moreover, the reported nonlinear absorption observed in those materials would arise as an effect of the negative refraction process (see the likeness for the transmittance results in Fig. 2 top and Fig. 2, bottom), but the only way to discriminate both effects is to measure R and T, simultaneously. Unfortunately, only the transmittance was measured in these works, which makes it difficult to give a definitive conclusion. Then, the Si and GaP would seem suitable as light-induced mirror devices, although more experimental research in this way is need.

To complete the previous analysis, we study the dependence of $\langle\epsilon_t\rangle$, T, R, and A on the dimensionless thickness $\tilde{d}$. The main results are summarized in Fig. 3, presented in matrix form as was Fig. 2. First, we analyze the limiting case $n_0\gamma=0$, where the light-induced free charge carriers do not affect the effective permittivity so that $\langle\epsilon_t\rangle=\epsilon_1$. This case is depicted in Fig. 3, top. Figure 3, top, left presents an attenuated oscillation of T exhibiting a decrease in average when the dimensionless thickness increases due to a greater medium energy absorption. This absorptive power improves because the photon mean path inside the medium also increases. On the other hand, R presents an oscillatory behavior without both attenuation and average change along the $\tilde{d}$ range. This fact indicates that the incident energy is only redistributed between T and A. The oscillatory behavior is a consequence of the well-known superposition process among counterpropagating forward and backward waves within the Fabry-Pérot geometry, i.e., it represents a modified *Airy-type pattern*. It was verified that the oscillation amplitude increases with increasing ϵ_1. The increment of the nonlinear conductivity coefficient $n_0\delta$ enhances both the T (A) average decreasing (increasing) along the $\tilde{d}$ range, ironing out their oscillatory behaviors. Also, in this case the R average is not affected by the thickness increment, showing that

the energy interchange occurs mainly between T and A. Figure 3, center shows the behavior for $n_0\gamma>0$. A marked oscillatory behavior in $\langle\epsilon_t\rangle$ is observed, which leads to marked oscillatory behavior of R, T, and A as function of $\tilde{d}$. Also, T (A), on average, decreases (increases), whereas R, on average, remains constant, being that oscillation is slightly dampened. In Fig. 3, center, left the oscillations in R, T, and A become bistable as $\tilde{d}$ increases. In addition, it was also verified that an increasing dimensionless thickness favors the bistable behavior since the bistable oscillations appear for lower ξ values. Moreover, when $\tilde{d}\ll 2\pi$, bistability does not occurs. On the other hand, when $n_0\delta$ increases, the oscillations are ironed out and the bistability disappears as Fig. 3, center, right shows. As it is expected, the R, T, and A oscillations are markedly dampened. It is interesting to observe that in average the behavior for R, T, and A is maintained for $n_0\gamma<0$ in spite of the $\langle\epsilon_t\rangle$ increasing in terms of $\tilde{d}$ as depicted in Fig. 3, bottom. However, note that the oscillations are almost eliminated, and thereby, the bistability does not appears even increasing the thickness and the excitation intensity. The monotonic behavior of R, T, and A is more marked for higher effective conductivity.

Finally, let us analyze the validity of the macroscopic-microscopic model considered. For the experimental situations related to light-induced free-charge-carrier media, it is observed that the macroscopic constants ϵ_t and σ_t present a linear dependence on the free-charge-carrier density. Therefore, the constitutive relations given by Eqs. (3) are general and capable of embracing the majority of experimental situations. However, as the nonlinear permittivity and conductivity are strongly dependent on the chosen microscopic model, a particular description would escape the scope of this paper. The reader interested in deepening in these questions can consult Ref. [35]. Our work basically deals with the macroscopic response of the media. Furthermore, the dependence of n on the dimensionless excitation parameter is considered by the microscopic processes related to one-photon interband transition. These processes were chosen because it has the main features of this kind of media. It should be pointed out that extensions to several other processes are very simple. For example, the case of extrinsic transitions is developed in Appendix and the similarities with the intrinsic case are remarked. Other processes, such as two-photon interband transitions and nonlinear intraband transitions, are not considered but could easily be included. In the studied case, fluctuations were disregarded and Eq. (4) should be seen as the equation for the most probable value of n [9]. For this reason, n_0 has a fixed value and no thermal excitation was included. This fact is justified because, in the most of the experimental cases, optical excitation overcomes thermal excitation in several orders of magnitude. On the other hand, for the relaxation, bimolecular recombination was used. This situation applies to cases where the carrier density is high and generated throughout the medium bulk for low-mobility materials [6]. This is the case of the experimental situations commonly found when the optical properties of light-induced free-charge-carrier media are concerned. Finally, we have disregarded diffusion of the induced free charge carriers along the z coordinate because in the experimental situations

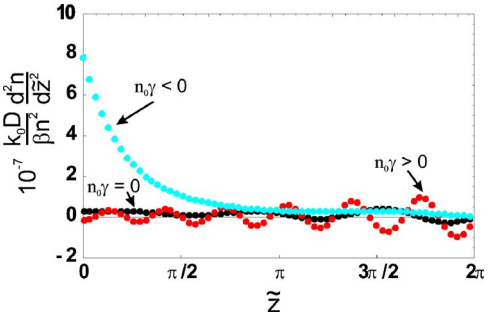

FIG. 4. (Color online) Ratio among the diffusion and recombination terms as a function of the dimensionless spatial coordinate for $n_0\gamma=0$, $n_0\gamma>0$, and $n_0\gamma<0$, as indicated in the figure, with $\epsilon_1=2.25$, $n_0\delta=10^{-4}$, $\xi=10^9$ and $\tilde{d}=2\pi$.

it can only contribute markedly for interferometrical excitation patterns with transversal submicron spatial variations. In our case, the longitudinal variations are smooth enough as to not interfere in the final result. In order to show that the diffusion is negligible in the studied case, we compare the recombination term in Eq. (4), $\beta n^2(\tilde{z})$, with the diffusion term $k_0 D d^2 n/d\tilde{z}^2$. Figure 4 depicts the ratio of both magnitudes as function of the dimensionless spatial coordinate $\tilde{z}$. This ratio should be compared to unity to know when diffusion is important. If a Langevin-type recombination [5] is considered, then $\beta=\theta\mu e/\epsilon_1$ with e the electron charge, μ the sum of the carrier mobility, and θ a constant that controls deviations from Langevin regime, $\theta\approx 1$. Besides, if the Einstein relation holds, $D=\mu kT$, where k is the Boltzman constant and T the absolute temperature, then at room temperature, it is expected that $k_0 D d^2 n/d\tilde{z}^2/(\beta n^2)\approx \mathbb{O}[10^{-7}]\ll 1$ for all $n_0\gamma$ values and $\tilde{d}=2\pi$, as shown in Fig. 4. This result was verified for higher values of $\tilde{d}$. Therefore, the diffusion could be a negligible process within the studied model so that it can be disregarded in the rate equation [Eq. (4)].

IV. CONCLUSIONS

We studied the wave propagation and optical properties of light-induced free-charge-carrier media by combining a microscopic and macroscopic model within a Fabry-Pérot framework. The variable that links both models is the time-averaged Poynting vector modulus, which can be directly monitored within the medium through the S-formalism. This approach replaces the traditional field equation by a coupled set of equations that includes the time-averaged Poynting vector modulus as the field variable. Then, the macroscopic-microscopic set of equations were numerically solved so that the transmittance, reflectance, absorptive power, and spatially averaged permittivity were obtained as a function of dimensionless excitation parameter and dimensionless thickness. The main results can be summarized as follows: (i) For the limiting case of a pure photoconductor characterized by $n_0\gamma=0$ and $\langle\epsilon_t\rangle=\epsilon_1$, the transmittance decreases monotonously on the dimensionless excitation parameter and almost all the incident energy is absorbed since the reflectance remains negligible. This behavior is enhanced for higher val-

ues of the nonlinear conductivity coefficient. In terms of dimensionless thickness, T decreases and A increases, both with an oscillatory behavior. This fact occurs because of the constructive and destructive superposition of forward and backward "waves" within the medium. The oscillation is ironed out when the nonlinear conductivity coefficient increases. (ii) For $n_0\gamma>0$, the behavior of T, R, and A is quite different. As the excitation intensity increases, T and R become oscillatory and, for higher ξ values, the oscillations become bistable, as a consequence of the bistable behavior of the effective permittivity. However, the increment of the nonlinear photoconductivity coefficient produce a quenching in the bistability, and the oscillations are strongly ironed out. Therefore, the absorptive power increment prejudices the bistability appearing for higher dimensionless excitation parameters values. On the other hand, when the dimensionless thickness is of concern, the T Airy-type pattern is damped by the nonlinear conductivity and becomes bistable when the slab thickness increases. However, the reflectance envelope does not change with the increment of that parameter. This implies that the radiation energy is only redistributed between T and A without change, on average, the reflectance. As it was expected, the absorptive power increment through the nonlinear coefficient irons out the oscillations and can quench the bistability. (iii) For $n_0\gamma<0$, the oscillations are strongly reduced or eliminated depending of the ϵ_1 value, and therefore, bistability disappears. There exist a value for the dimensionless excitation parameter from which the spatially averaged permittivity becomes lower than the unity, producing a decrease in the absorptive power and the transmittance while the reflectance experiences a sudden increase. Thus, by increasing ξ even more, the reflectance approximates to the unity $R\approx 1$. Also, the reflectance remains quasi-invariant as far as the thickness increases. This result enables the possibility of building light-induced mirror devices that could be used as photonic or optoelectronic components in optical integrated circuits, and also as optical limiters. Finally, we remark that is not enough to analyze the transmittance behavior to characterize a nonlinearity because this is not sufficient to distinguish some types of nonlinearities, such as, for example, pure nonlinear absorption ($\gamma n_0=0$) and negative nonlinear permittivity ($\gamma n_0<0$). Reflectance analysis is also necessary. In fact, some techniques used to characterize nonlinearities based only on transmittance analysis [36] would not be sufficient.

ACKNOWLEDGMENT

A.L. acknowledges CLAF-CNPq for financial support.

APPENDIX: MICROSCOPIC PROCESSES FOR EXTRINSIC TRANSITIONS

In this appendix, we briefly review the microscopic processes that appear in extrinsic n-type transitions and calculate the form for the induced free-charge-carrier density. Referring to Fig. 5, there exist a density N_D of donor centers, which in absence of optical excitation can be already excited (N_{D+}) both in the conduction band giving a free-charge-carrier density n_0 or trapped in acceptor centers N_A that does not interact with the light. Under optical excitation, some of the available centers (N_D-N_{D+}) goes to the conduction band with probability α; then, it can be recombined by $N_{D+}n$ with probability β. Therefore, the rate equation that describes this processes is

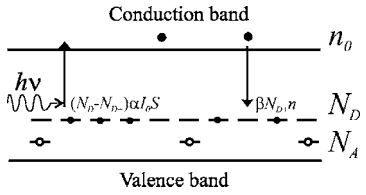

FIG. 5. Schematic representation of the extrinsic n-type transitions problem. Electrons are excited from donors centers N_D to begin a free carrier electron.

$$\frac{dn}{dt} = (N - N_{D+})\alpha I_o S - \beta N_{D+} n, \tag{A1}$$

where the spatial and temporal dependence were omitted by simplicity. The neutrality of the medium imposes the condition

$$N_{D+} = n + n_0 + N_A. \tag{A2}$$

Then, for $d/dt=0$, Eq. (A1) (with the above condition) solves to

$$\frac{n(z)}{(n_0+N_A)} = \frac{\xi' S(z)+1}{2}\left(\sqrt{1+\frac{4(N_{0A}-1)\xi' S(z)}{[\xi' S(z)+1]^2}}-1\right), \tag{A3}$$

where $\xi' = \alpha I_o/[\beta(n_0+N_A)]$ is the extrinsic dimensionless excitation parameter and $N_{0A}=N/(n_0+N_A)$ is the extrinsic relative density of atoms. This expression is known for photorefractive materials [37] and, in general, for extrinsic semiconductors [9]. Then, for extrinsic transitions also the fractional density of light-induced free charge carriers can be studied in terms of only two dimensionless parameters: ξ' and N_{0A}. Since for all practical purposes $\xi' \gg 1$, the functional behavior of Eq. (A3) is equal to that of Eq. (5). Then, the results obtained for intrinsic interband transition processes can be applied also for extrinsic transitions.

[1] T. F. Boggess, S. C. Moss, I. W. Boyd, and A. L. Smirl, Opt. Lett. **9**, 291 (1984).
[2] T. F. Boggess, Jr., A. L. Smirl, S. C. Moss, I. W. Boyd, and E. W. Van Stryland, IEEE J. Quantum Electron. **QE-21**, 488 (1985).
[3] A. I. Ryasnyanskiy, Proc. SPIE **5640**, 179 (2004).
[4] D. L. Smith, J. Appl. Phys. **53**, 7051 (1982).
[5] R. H. Young, J. Appl. Phys. **60**, 272 (1988).
[6] I. Chen, J. Appl. Phys. **49**, 1162 (1978).
[7] E. Theocharous, J. Ishii, and N. P. Fox, Appl. Opt. **43**, 4182 (2004).
[8] R. A. Smith, Appl. Opt. **4**, 631 (1965).
[9] T. J. Brukilacchio, M. D. Skeldon, and R. W. Boyd, J. Opt. Soc. Am. B **1**, 354 (1984).
[10] M. di Domenico, Jr., W. M. Sharpless, and J. J. McNicol, Appl. Opt. **4**, 677 (1965).
[11] E. H. Putley, Appl. Opt. **4**, 649 (1965).
[12] M. Gao, S. Kapplan, R. Pankrath, X. Feng, Y. Tang, and V. Vikhnin, J. Phys. Chem. Solids **61**, 1775 (2000).
[13] L. Mosquera, I. de Oliveira, J. Frejlich, A. C. Hernandes, S. Lafrendi, and J. F. Carvalho, J. Appl. Phys. **90**, 2635 (2001).
[14] K. Takizawa, M. Okada, H. Kikuchiand, and T. Aida, Appl. Phys. Lett. **53**, 2359 (1988).
[15] A. E. Attard, Appl. Opt. **28**, 5169 (1989); R. C. Hughes and R. J. Sokel, J. Appl. Phys. **52**, 6743 (1981).
[16] P. Dittrich, B. Koziarska-Glinka, G. Montemezzani, P. Günter, S. Takekawa, K. Kitamura, and Y. Furukawa, J. Opt. Soc. Am. B **21**, 632 (2004).
[17] H. Zeng, C. Liu, S. Tokura, M. Kira, and Y. Segawa, Chem. Phys. Lett. **331**, 71 (2000).
[18] R. C. Hughes, Appl. Phys. Lett. **21**, 196 (1972).
[19] H. Haug and S. W. Koch, *Quantum Theory of the Optical and Electronic Properties of Semiconductors*, 3rd ed. (World Scientific, Singapore, 1998), pp. 274.
[20] R. H. Bube, *Photoconductivity of Solids*, 2nd ed. (Wiley, New York, 1967), p. 326.
[21] L. W. Tutt and T. F. Boggess, Prog. Quantum Electron. **17**, 299 (1993).
[22] A. Lencina and P. Vaveliuk, Phys. Rev. E **71**, 056614 (2005).
[23] W. Chen and D. L. Mills, Phys. Rev. B **35**, 524 (1987).
[24] See, for example, Ref. [19], pp. 1–16.
[25] D. H. Auston, S. Mc Afee, C. V. Shank, E. P. Ippen, and O. Teschke, Solid-State Electron. **21**, 147 (1978).
[26] R. S. Hansen, Appl. Opt. **42**, 4819 (2003).
[27] A. Carbone and P. Mazzetti, Phys. Rev. B **49**, 7592 (1994).
[28] The absorptive power is defined as the fraction that the body absorbs of the radiant energy which falls upon it in Ref. [29].
[29] M. Born and E. Wolf, *Principles of Optics* 7th reprinted ed. (Cambridge University Press, Cambridge, England, 2003), p. 747.
[30] There is a large amount of experimental data for semiconductors and photoconductors located at http://www.ioffe.rssi.ru/SVA/NSM
[31] D. A. B. Miller, S. D. Smith, and A. Johnston, Appl. Phys. Lett. **35**, 658 (1979).
[32] C. D. Poole and E. Garmire, Appl. Phys. Lett. **44**, 363 (1984).
[33] T. F. Boggess, S. C. Moss, I. W. Boyd, and A. L. Smirl, Opt. Lett. **9**, 291 (1984).
[34] S. J. Rychnovsky, G. R. Allan, C. H. Venzke, A. L. Smirl, and T. F. Boggess, Proc. SPIE **1692**, 191 (1992).
[35] See, for example, Ref. [19], Chap. 5.
[36] M. Sheik-Bahae, A. A. Said, T. H. Wei, D. J. Hagan, and E. W. Van Stryland, IEEE J. Quantum Electron. **QE-26**, 760 (1990); J. Jayabalan, A. Singh, and S. M. Oak, Appl. Opt. **45**, 3852 (2006).
[37] P. Vaveliuk, B. Ruiz, and N. Bolognini, Phys. Rev. B **59**, 10985 (1999); P. Vaveliuk, B. Ruiz, O. Martinez Matos, G. A. Torchia, and N. Bolognini, IEEE J. Quantum Electron. **37**, 1040 (2001).